

Supporting Information

2 Global Chemical Composition of Ambient Fine Particulate Matter for Exposure

3 Assessment

4 Sajeev Philip^{1*}, Randall V. Martin^{1, 2}, Aaron van Donkelaar¹, Jason Wai-Ho Lo¹, Yuxuan Wang³,
5 Dan Chen⁴, Lin Zhang⁵, Prasad S. Kasibhatla⁶, Siwen Wang⁷, Qiang Zhang⁸, Zifeng Lu⁹, David
6 G. Streets⁹, Shabtai Bittman¹⁰ and Douglas J. Macdonald¹¹

7

⁸ ¹Department of Physics and Atmospheric Science, Dalhousie University, Halifax, Nova Scotia,
⁹ Canada

¹⁰ ²Also at Harvard-Smithsonian Center for Astrophysics, Cambridge, Massachusetts, USA

¹¹ Ministry of Education Key Laboratory for Earth System Modeling, Center for Earth System
¹² Science, Institute for Global Change Studies, Tsinghua University, Beijing, China

13 ⁴Department of Atmospheric and Oceanic Sciences, University of California, Los Angeles,
14 California, USA.

¹⁵Department of Atmospheric and Oceanic Sciences, School of Physics, Peking University, China

¹⁶ Nicholas School of the Environment and Earth Sciences, Duke University, Durham, North
¹⁷ Carolina, USA.

18 ⁷State Key Joint Laboratory of Environment Simulation and Pollution Control, School of
19 Environment, Tsinghua University, Beijing, China.

²⁰Center for Earth System Science, Tsinghua University, Beijing, China.

²¹ ⁹Decision and Information Sciences Division, Argonne National Laboratory, Argonne, IL, USA

22 ¹⁰Agriculture and Agri-Food Canada, Agassiz, British Columbia, Canada

23 ¹¹Environment Canada, Canada

24

25 **Author Information**

26 Corresponding Author

27 *Phone: +19024941820; Fax: +19024945191; e-mail: philip.sajeev@dal.ca

28

29 This file contains 23 Pages with 5 Figures and 2 Tables.

30

31 **Description of the GEOS-Chem aerosol simulation**

32 We used the GEOS-Chem global three-dimensional chemical transport model (version 9-01-03;
33 <http://geos-chem.org>) to calculate the local conversion factors (ratio of component to AOD)
34 coincident with each satellite observation of AOD. The GEOS-Chem uses assimilated
35 meteorological data from the Goddard Earth Observing System (GEOS-5) at the NASA Global
36 Modeling Assimilation Office (GMAO). The meteorological data includes instantaneous fields,
37 surface variables (e.g., mixed layer depth) at a temporal resolution of 3 hours, and other variables
38 at 6 hours. We reduced the stratospheric layers of the native GEOS-5 vertical grids (72 hybrid
39 eta levels) to 48 for computational expediency. The vertical layers of the current model extend
40 from the Earth's surface to the top of the atmosphere (0.01 hPa) with 47 vertical levels. The
41 lowest layer of the model is centered at approximately 70 meters, and used here to represent the
42 ground-level aerosol concentrations.

43 The native horizontal resolution for the GEOS-5 meteorological data is $0.5^{\circ} \times 0.667^{\circ}$. First, we
44 used data regridded to a coarser resolution of $2^{\circ} \times 2.5^{\circ}$ for computational expediency, and
45 performed the global simulation at this resolution. Second, we conducted three regional (nested)
46 simulations at the native horizontal resolution of $0.5^{\circ} \times 0.667^{\circ}$ for three regions of the globe:
47 North America (140°W – 40°W , 10°N – 70°N), Europe (30°W – 50°E , 30°N – 70°N) and East Asia
48 (70°W – 150°W , 11°S – 55°N). This higher resolution simulation preserves the finer spatial patterns
49 of the chemical components (1, 2). The global simulation outputs were used as boundary
50 conditions for the regional grids. We spun up the model for one month before each global and
51 regional simulation to remove the effects of initial conditions on the aerosol simulation. The
52 dynamical processes (transport and convection) have a temporal resolution of 10 minutes for the
53 nested simulations and 15 minutes for the global simulation. We used a timestep of 60 minutes
54 for chemical processes and emissions for both nested and global resolutions. We used full
55 mixing of species below the mixed layer, with a correction to the GEOS-5 predicted nocturnal
56 mixed layer depth as described in Heald et al. (3) and Walker et al. (4).

57 GEOS-Chem simulates HO_x - NO_x -VOC-ozone-aerosol chemistry in detail (5, 6). Park et al. (6)
58 describe the simulation of secondary inorganic ions coupled to gas phase chemistry. The
59 simulation of aerosol-gas interactions are through the aerosol extinction effects on photolysis
60 rates (7), and heterogeneous chemistry (8) with updated N_2O_5 (9) and HO_2 (10) uptake by
61 aerosols. The ISORROPIA II thermodynamic scheme (11) is used for partitioning gases and
62 aerosols (12). GEOS-Chem uses in-cloud sulfate formation using the cloud liquid water content
63 and cloud volume fractions of the GEOS-5 data (13). We artificially limited the nitric acid to two
64 thirds of its value for each timestep to correct for an overestimation in HNO_3 found in
65 comparison with measurements over the eastern U.S. (3). GEOS-Chem calculates AOD based on

66 the relative humidity dependent aerosol optical properties as described in Martin et al. (7) with
67 an updated growth factor for organic matter, and updates to ammonium sulfate optics.
68 Modification to dust optics is described in Ridley et al. (14).

69 The GEOS-Chem simulation uses emission inventories of aerosol and its precursor gases as
70 input. We used regional anthropogenic emission inventories of NO_x and SO₂ over Canada (CAC;
71 <http://www.ec.gc.ca/inrp-npri/>), the U.S. (Environmental protection Agency-National Emissions
72 Inventory 2005; <http://www.epa.gov/ttnchie1/net/2005inventory.html>), Mexico (BRAVO;(15)),
73 Europe (EMEP; <http://www.emep.int/>), and East Asia ((16) for NO_x; (17) for SO₂. Elsewhere,
74 we used anthropogenic emissions from EDGAR v32-FT2000 global inventory for 2000 (18), and
75 scaled it based on the energy statistics to subsequent years (19). Anthropogenic NO_x emissions
76 were scaled from 2006 to subsequent years based on the NO₂ column density data retrieved from
77 the OMI satellite sensor (20). GEOS-Chem includes soil NO_x (21, 22), lightning NO_x (23-27),
78 ship SO₂ from the ICOADS inventory (28, 29), and volcanic emissions (13). Seasonality for NO_x
79 and SO₂ is based on the statistics from regional inventories. GEOS-Chem includes a diurnal
80 variation for NO_x as described in van Donkelaar et al. (19). Global ammonia emission in GEOS-
81 Chem is from Bouwman et al. (30) with a seasonality imposed by Park et al. (6). Spatial and
82 seasonal NH₃ variation over Canada is based on monthly varying agricultural activity statistics
83 provided by the Agriculture Canada (31). Other regional inventories are over the U.S. (EPA-
84 NEI), Europe (EMEP), and East Asia (32). East Asian annual emissions are superimposed with a
85 relative seasonal variation (13, 33), and a reduction of 30% (33) motivated by comparison with
86 other inventories (34, 35). We doubled NH₃ emissions over California as suggested by Heald et
87 al. (3) and Walker et al. (4).

88 GEOS-Chem carbonaceous aerosols include black carbon (BC), organic carbon (OC), and
89 secondary organic aerosols (SOA) (3, 36, and 37). The global anthropogenic OC and BC
90 inventory is from Bond et al. (38), with the Cooke et al. (39) inventory over North America (40),
91 and the Lu et al. (17) inventory over East Asia. We doubled the East Asian OC and BC
92 emissions based on a comparison with top-down inversion of regional inventories by Fu et al.
93 (41) and recognize there is ongoing discussion on this topic (42). GEOS-Chem simulates the
94 formation of SOA from the oxidation of volatile organic compounds (43-46). Global biomass
95 burning emission is from the GFED-3 inventory at 3-day temporal resolution (47, 48), and global
96 biofuel emission is from Yevich and Logan (49) superimposed with the regional inventories
97 mentioned above. We calculated OM as the sum of model OC and SOA. We used the OM/OC
98 ratio estimated from observations by the OMI satellite sensor and Aerosol Mass Spectrometer to
99 convert OC to OM to account for the presence of non-carbon elements (50).

100 GEOS-Chem includes the simulation of natural particles such as mineral dust and sea salt. The
101 mineral dust simulation is described by Fairlie et al. (51). We used the first dust size bin and 37%
102 of the second dust size bin (out of the 4 bins) to get a PM_{2.5} size range. Sea salt emission in the
103 model is described by Alexander et al. (52) with updates by Jaegle et al. (53). We use sea salt
104 accumulation mode size range from 0.1 to 1 μm , which in normal coastal conditions represents
105 the approximate PM_{2.5} size range.

106 GEOS-Chem includes dry deposition (22), and wet deposition (37, 54, 55).

107 Numerous studies have evaluated the GEOS-Chem ground-level aerosol concentrations and its
108 seasonal variation (e.g., 3, 4, 6, 12, 36, 40, 41, 51, 56, and 57). Vertical profiles of aerosol
109 composition were also compared with various aircraft observations (e.g., (19, 58, 59), and with

110 CALIOP satellite observations (60-62). Six-year coincident comparisons of GEOS-Chem and
111 CALIOP suggest simulated near-surface to column extinction ratios are often within 25%, but
112 can approach a factor of two in certain seasons and locations (61).

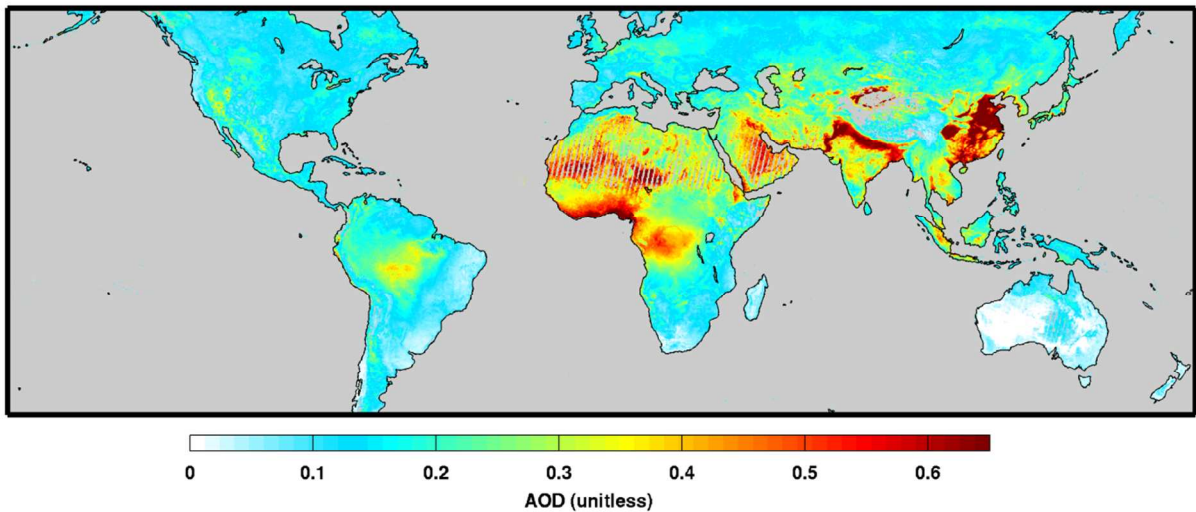
113 **Description of the ground-based PM_{2.5} composition measurements**

114 We utilized filter-based in situ measurements by several networks, such as, the National Air
115 Pollution Surveillance Network (NAPS) and the Canadian Air and Precipitation Monitoring
116 Network (CAPMoN) over Canada (<http://www.on.ec.gc.ca/natchem>). The U.S. measurement
117 networks include the Clean Air Status and Trends Network (CASTNET,
118 http://java.epa.gov/castnet/epa_jsp/sites.jsp), the Interagency Monitoring of Protected Visual
119 Environments (IMPROVE, <http://vista.cira.colostate.edu/improve/>), and the U.S.
120 Environmental Protection Agency Air Quality System (EPA-AQS,
121 <http://www.epa.gov/ttn/airs/airsaqs/>). The NAPS network provides 24-hr composition every
122 third day across Canada as described in Dabek-Zlotorzynska et al. (63). We used weekly average
123 sulfate and ammonium ion measurements from the CAPMoN and the CASTNET networks even
124 though they are devoid of PM_{2.5} filters (64). The IMPROVE network provides 24-hr PM_{2.5}
125 composition data except for ammonium for every third day from several national parks in the
126 U.S. The EPA-AQS network mainly operates over rural areas which report 24-hr averages of all
127 the major composition measurements every consecutive third or sixth day. Here, we used the
128 PM_{2.5} composition data from EPA-AQS and IMPROVE networks (2005-2008 mean) reported by
129 Hand et al. (65). We calculated ammonium from sulfate and nitrate measurements of EPA-AQS
130 and IMPROVE networks by assuming a fully neutralized sulfuric acid by ammonia gas. We
131 averaged the data reported by Hand et al. (65), and the long-term (2004-2008) in situ

132 measurements from other networks into the $0.1^{\circ} \times 0.1^{\circ}$ grid for comparison with satellite-model
133 composition over North America.

134 We treated these in situ data as ‘truth’ to evaluate our product. However, it is worth noting some
135 uncertainties. Carbon measurements are prone to errors due to filter contamination (e.g., 66). The
136 ratio of OM to OC varies from 1.2 to 2.6 depending on the spatial and seasonal differences (e.g.,
137 67, 68). Mineral dust concentrations were from the elemental measurements of IMPROVE and
138 EPA-AQS following Malm et al. (69) even though measurements of five elements alone are
139 inadequate to determine the ambient mineral dust (65, 70). Sea salt were from elemental chlorine
140 or chlorine ion measurements, by accounting for 55% chlorine by weight; the selection of sea
141 salt marker as sodium or chlorine is also uncertain (65, 71). Hand et al. (72) obtained relative
142 errors for PM_{2.5} and its chemical components from a comparison of collocated IMPROVE and
143 AQS measurements (17% for PM_{2.5}, 5% for ammonium sulfate, 11% for ammonium nitrate, 10%
144 for OC, 12% for EC, 33% for dust, and 77% for sea salt). Finally, the gridded in situ data are
145 prone to representation error as an individual measurement is used to represent a 10 km x 10 km
146 area.

147 In addition, we collected annually representative inorganic and organic composition
148 measurements from the European Monitoring and Evaluation Programme (EMEP;
149 <http://www.emep.int/>), the Acid Deposition Monitoring Network in East Asia (EANET;
150 <http://www.eanet.cc/>), and several field measurements around the world from published papers
151 e.g., (41, 73, 74) (for organic measurements) and several others (Table S2). We used this dataset
152 to evaluate the global satellite-model composition. We included only sites with all SIA
153 components to achieve a consistent evaluation.



154

155 **Figure S1.** Combined aerosol optical depth (AOD) from the MODIS and MISR satellite
156 instruments for 2004-2008. Gray denotes water or missing satellite AOD observations.

157

158

159

160

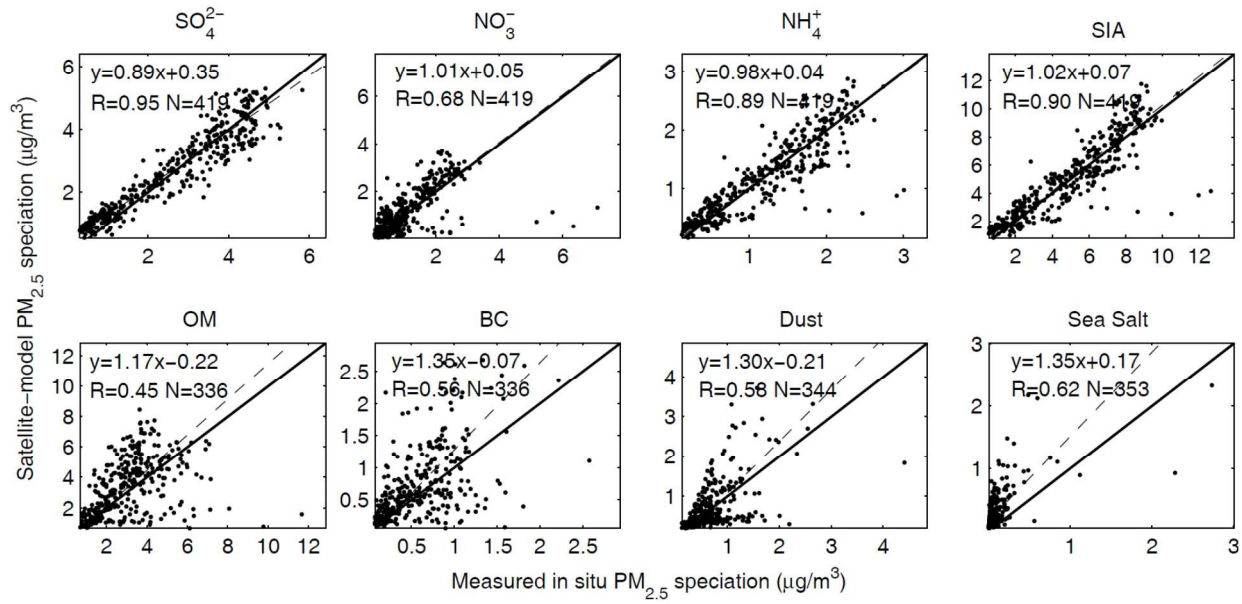
161

162

163

164

165



166

167 **Figure S2.** Comparison of PM_{2.5} composition from the satellite-model product versus in situ
 168 observations across North America. The solid black line is the 1:1 line, and the dashed line is the
 169 best fit line. The inset contains the Pearson correlation coefficient as well as the slope and
 170 intercept from reduced major axis regression.

171

172

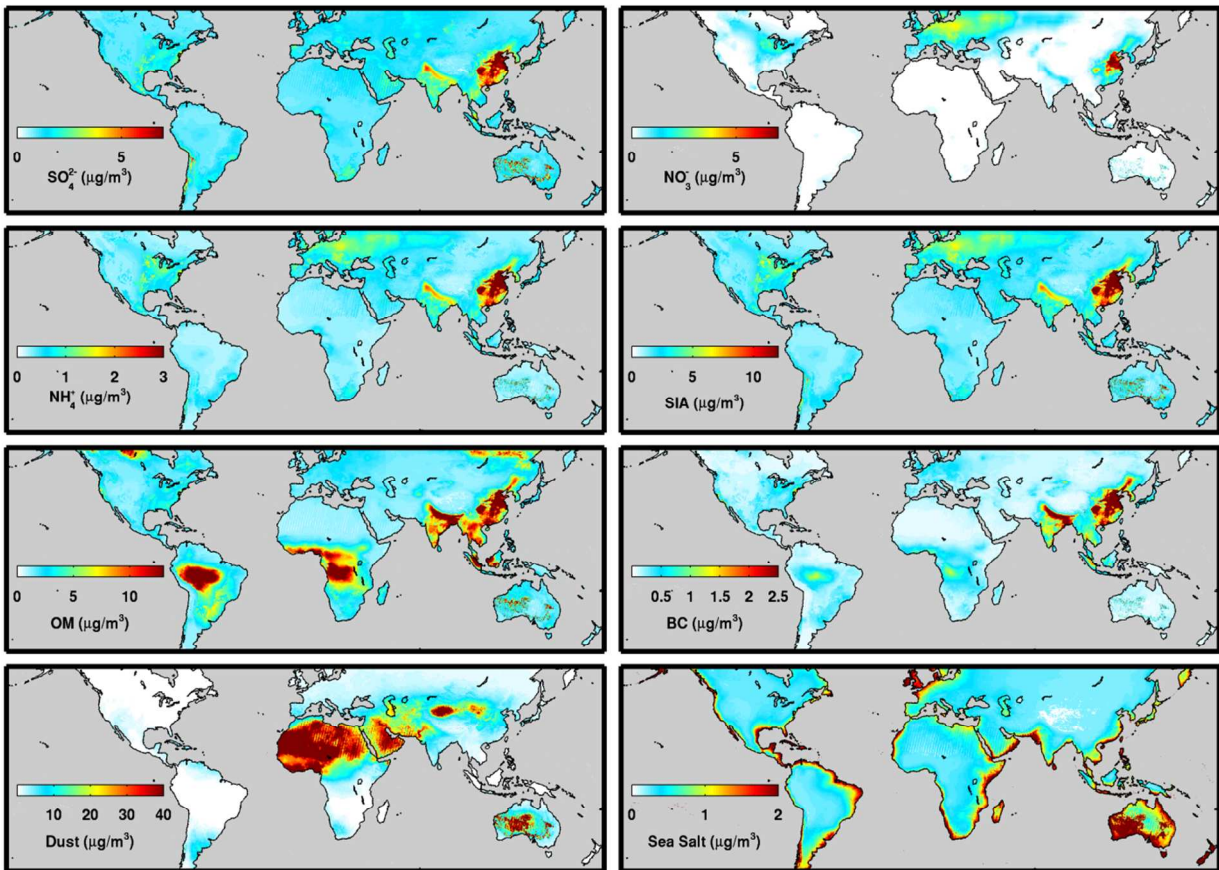
173

174

175

176

177



178

179 **Figure S3.** Absolute uncertainty of satellite-model $\text{PM}_{2.5}$ composition determined by propagation
180 of error. Gray denotes water.

181

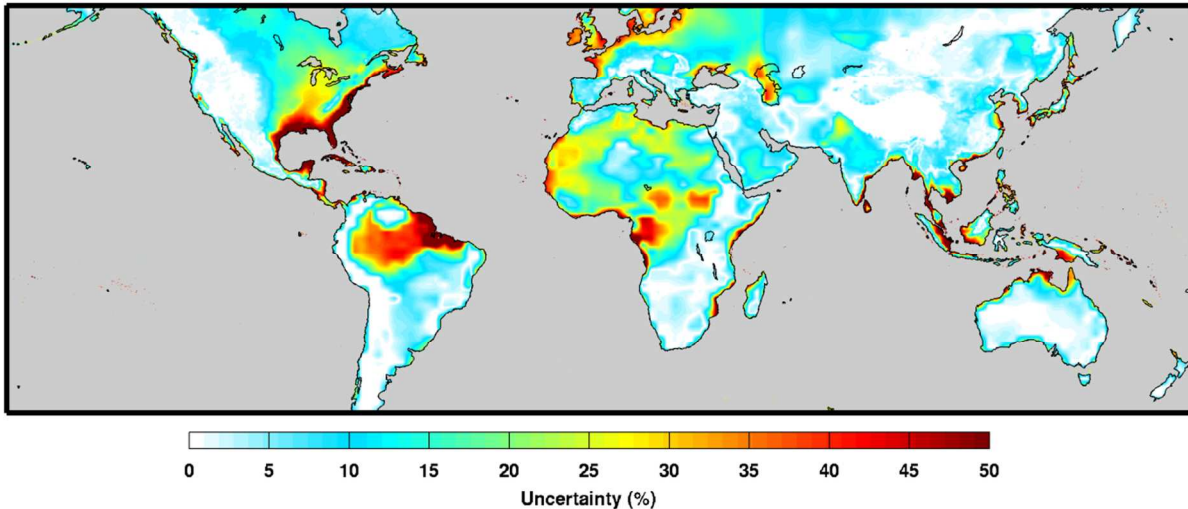
182

183

184

185

186



187

188 **Figure S4.** Uncertainty in $\text{PM}_{2.5}$ due to GEOS-Chem model vertical profile bias determined by
189 comparison with CALIOP satellite observations of aerosol extinction following van Donkelaar et
190 al. (61). Gray denotes water.

191

192

193

194

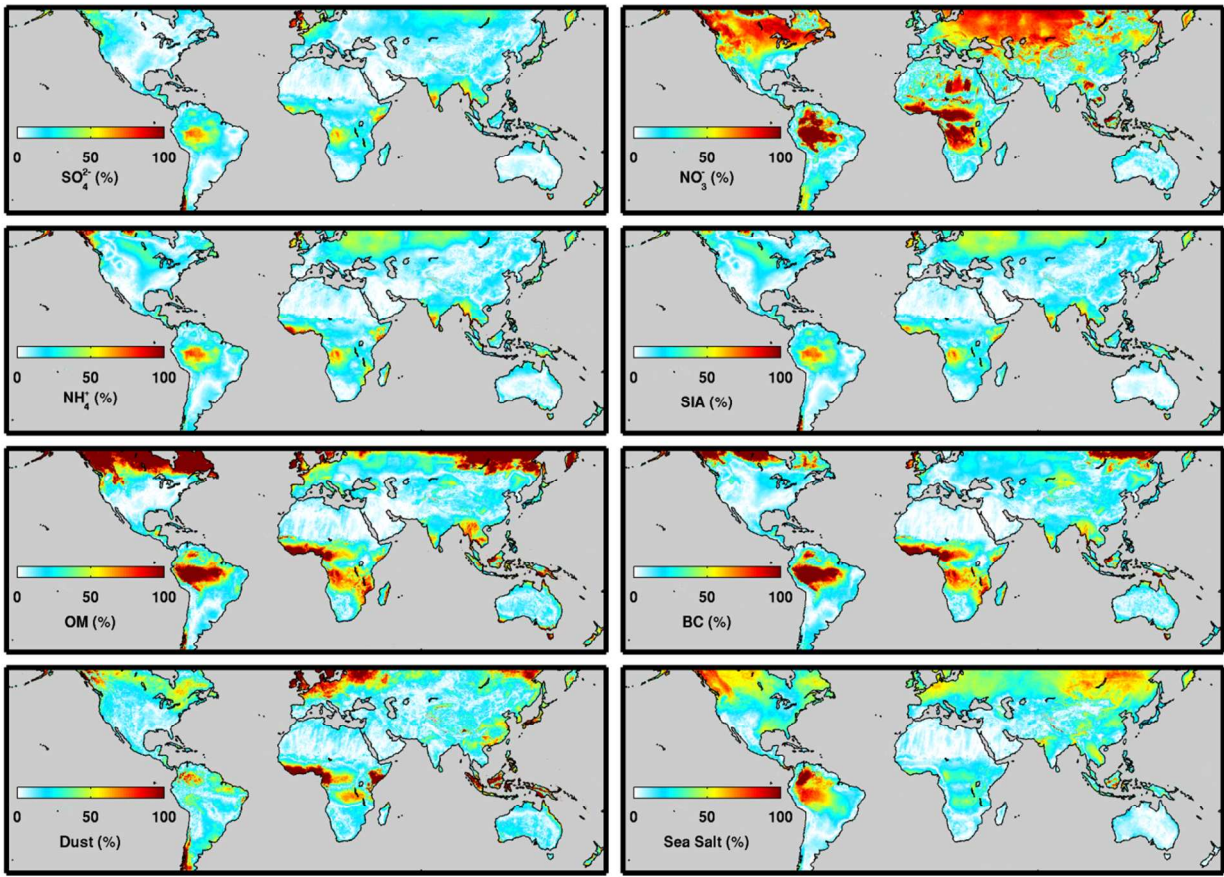
195

196

197

198

199



200

201 **Figure S5.** Uncertainty in satellite-model PM_{2.5} composition due to incomplete sampling
 202 estimated as the difference between the long-term mean simulated PM_{2.5} composition sampled
 203 continuously versus coincidentally with the satellite observations. Gray denotes water.

204

205

206

207

208

PM _{2.5} Composition	Data	North America				Global			
		r	Slope	Offset ($\mu\text{g}/\text{m}^3$)	N	r	Slope	Offset ($\mu\text{g}/\text{m}^3$)	N
SO_4^{2-}	Satellite	0.95	0.89	0.35	419	0.92	0.88	0.93	55
	Simulation	0.97	0.73	0.23	419	0.94	0.61	0.80	55
NO_3^-	Satellite	0.68	1.01	0.05	419	0.73	0.83	-0.26	55
	Simulation	0.63	0.80	0.11	419	0.69	0.64	-0.24	55
NH_4^+	Satellite	0.89	0.98	0.04	419	0.92	1.08	0.13	55
	Simulation	0.89	0.79	0.04	419	0.93	0.77	0.12	55
SIA	Satellite	0.90	1.02	0.07	419	0.93	0.91	0.85	55
	Simulation	0.90	0.82	0.10	419	0.92	0.64	0.70	55
OM	Satellite	0.45	1.17	-0.22	336	0.67	0.42	-0.73	56
	Simulation	0.42	0.99	-0.34	336	0.61	0.30	-0.47	56
BC	Satellite	0.56	1.35	-0.07	336	0.65	1.05	-1.83	65
	Simulation	0.53	1.04	-0.04	336	0.56	0.68	-1.15	65

209

210 **Table S1.** Comparison of PM_{2.5} composition from the simulation and satellite-model product
 211 versus in situ observations across North America, and globally (non-North American).
 212 Abbreviations are Secondary Inorganic Aerosol (SIA; the sum of SO_4^{2-} , NO_3^- and NH_4^+), Organic
 213 Mass (OM), and Black Carbon (BC). “Satellite” and “Simulation” in the second column
 214 represents satellite-model composition, and complete model simulation respectively at a spatial
 215 resolution of 0.1° x 0.1°. Correlation statistics are calculated with reduced major axis regression.

216

217

218

219

Sl. No.	Site/City	Country	Latitude	Longitude	Study Period	SO_4^{2-}	NO_3^-	NH_4^+	OC	BC	Size	Source
						degree	degree	$\mu\text{g}/\text{m}^3$	$\mu\text{g}/\text{m}^3$	$\mu\text{g}/\text{m}^3$	$\mu\text{g}/\text{m}^3$	$\mu\text{g}/\text{m}^3$
1	Beijing	China	40.3	116.3	Mar 2005 - Feb 2006	15.8	10.1	7.3	34.4	8.3	PM _{2.5}	75
2	Miyun Reservoir	China	40.5	116.8	Mar 2005 - Feb 2006	13.0	6.4	6.1	21.9	3.8	"	"
3	Chongqing	China	29.6	106.5	Mar 2005 - Feb 2006	25.5	5.3	7.9	42.2	6.5	"	"
4	Dadukou	China	29.5	106.5	Mar 2005 - Feb 2006	23.4	5.1	7.6	47.2	6.4	"	"
5	Jinyun	China	29.8	106.4	Mar 2005 - Feb 2006	24.0	4.8	7.3	41.2	4.7	"	"
6	Hok Tsui	Hong Kong	22.2	114.3	Nov 2004 - Oct 2005	11.9	0.8	3.1	4.3	2.1	"	76
7	Tsuen Wan	Hong Kong	22.4	114.1	Nov 2004 - Oct 2005	13.2	1.6	4.1	7.4	6.0	"	"
8	Mong Kok	Hong Kong	22.3	114.1	Nov 2004 - Oct 2005	12.8	2.4	4.4	11.9	13.7	"	"
9	Delhi	India	28.4	77.1	Mar 2001 - Jan 2002	10.9	6.1	6.4	40.3	10.5	"	77
10	Mumbai	India	22.6	88.3	Mar 2001 - Jan 2002	6.9	1.6	2.0	12.6	4.6	"	"
11	Kolkata	India	18.7	72.8	Mar 2001 - Jan 2002	7.2	2.9	3.6	37.1	12.1	"	"
12	Lahore	Pakistan	31.5	74.3	Jan 2007 - Jan 2008	10.5	6.6	3.6	64.4	11.2	"	78
13	Brazil	Brazil	23.0	43.2	Sep 2003 - Sep 2004	1.5	0.3	0.6	NA	2.1	"	79
14	Brazil	Brazil	22.9	43.2	Sep 2003 - Sep 2004	1.9	0.4	0.7	NA	3.1	"	"
15	Brazil	Brazil	22.9	43.2	Sep 2003 - Sep 2004	2.2	0.5	0.7	NA	2.9	"	"
16	Brazil	Brazil	23.0	43.4	Sep 2003 - Sep 2004	1.4	0.3	0.4	NA	1.3	"	"
17	Brazil	Brazil	23.0	43.3	Sep 2003 - Sep 2004	1.8	0.5	0.5	NA	2.7	"	"
18	Brazil	Brazil	22.8	43.4	Sep 2003 - Sep 2004	1.5	0.4	0.5	NA	3.2	"	"
19	Brazil	Brazil	23.0	43.6	Sep 2003 - Sep 2004	1.5	0.4	0.5	NA	1.2	"	"
20	Brazil	Brazil	22.9	43.6	Sep 2003 - Sep 2004	1.7	0.4	0.6	NA	2.4	"	"
21	Brazil	Brazil	22.9	43.4	Sep 2003 - Sep 2004	1.7	0.4	0.6	NA	2.5	"	"
22	Brazil	Brazil	22.9	43.7	Sep 2003 - Sep 2004	1.7	0.3	0.5	NA	1.7	"	"
23	Tel Aviv	Israel	32.1	34.8	Jan 2007 - Dec 2007	5.2	0.7	NA	4.7	1.5	"	80
24	Haifa	Israel	32.8	35.0	Jan 2007 - Dec 2007	5.2	1.4	NA	3.0	1.0	"	"
25	W. Jerusalem	Israel	31.8	35.2	Jan 2007 - Dec 2007	4.6	1.0	NA	4.1	1.1	"	"
26	Hebron	Palestine	31.5	35.1	Jan 2007 - Dec 2007	3.8	0.9	NA	5.3	1.8	"	"
27	E. Jerusalem	Palestine	31.8	35.2	Jan 2007 - Dec 2007	4.4	0.9	NA	5.2	2.2	"	"
28	Nablus	Palestine	32.2	35.2	Jan 2007 - Dec 2007	4.3	1.0	NA	8.2	5.6	"	"
29	Amman	Jordan	32.0	35.8	Jan 2007 - Dec 2007	4.5	1.0	NA	6.2	2.4	"	"
30	Balearic islands	Spain	39.6	2.6	Jan 2004 - Feb 2005	3.9	0.9	2.0	2.9	0.5	"	81
31	Kuwait	Kuwait	29.3	48.0	Feb 2004 - Jan 2005	9.9	1.8	NA	3.7	2.5	"	82
32	Chengdu	China	30.7	104.0	Jan 2006 - Dec 2007	40.5	NA	14.0	36.3	10.8	PM ₁₀	83
33	Dalian	China	38.9	121.6	Jan 2006 - Dec 2007	23.3	NA	7.7	20.2	5.3	"	"
34	Dunhuang	China	40.2	94.7	Jan 2006 - Dec 2007	6.6	NA	0.4	26.7	3.6	"	"
35	Gaolanshan	China	36.0	105.9	Jan 2006 - Dec 2007	16.7	NA	6.5	19.1	3.8	"	"
36	Gucheng	China	39.1	115.8	Jan 2006 - Dec 2007	35.5	NA	14.4	38.5	11.0	"	"
37	Jinsha	China	29.6	114.2	Jan 2006 - Dec 2007	26.6	NA	7.6	15.3	3.0	"	"
38	Lhasa	China	29.7	91.1	Jan 2006 - Dec 2007	2.9	NA	0.2	21.7	3.8	"	"
39	LinAn	China	30.3	119.7	Jan 2006 - Dec 2007	21.7	NA	6.8	15.1	4.3	"	"
40	Longfengshan	China	44.7	127.6	Jan 2006 - Dec 2007	10.0	NA	2.5	15.9	2.3	"	"
41	Nanning	China	22.8	108.4	Jan 2006 - Dec 2007	21.6	NA	5.8	17.9	4.0	"	"
42	Panyu	China	23.0	113.4	Jan 2006 - Dec 2007	26.8	NA	8.6	22.3	7.9	"	"
43	Taiyangshan	China	29.2	111.7	Jan 2006 - Dec 2007	28.8	NA	7.9	13.8	2.7	"	"
44	Xian	China	34.4	109.0	Jan 2006 - Dec 2007	46.7	NA	14.4	42.6	12.7	"	"
45	Zhengzhou	China	34.8	113.7	Jan 2006 - Dec 2007	45.0	NA	16.5	29.2	9.2	"	"
46	Akdala	China	47.1	88.0	Jul 2004 - Mar 2005	3.3	NA	0.6	2.9	0.4	"	84,85
47	Shangri-La, Zhuzhang	China	28.0	99.7	Jul 2004 - Mar 2005	1.6	NA	0.2	3.1	0.3	"	"

220 **Table S2.** Global in situ data collected from publications. "NA" represents data not available or
 221 filtered out.
 222
 223

224 **References**

225

- 226 1. Chen, D.; Wang, Y.; McElroy, M.B.; He, K.; Yantosca, R.M.; Le Sager, P. Regional CO
227 pollution and export in China simulated by the high-resolution nested-grid GEOS-Chem model.
228 *Atmospheric Chemistry and Physics* **2009**, 9 (11).
- 229 2. van Donkelaar, A.; Martin, R.V.; Pasch, A.N.; Szykman, J.J.; Zhang, L.; Wang, Y.X.; Chen,
230 D. Improving the Accuracy of Daily Satellite-Derived Ground-Level Fine Aerosol Concentration
231 Estimates for North America. *Environ. Sci. Technol.* **2012**, 46 (21), 11971-11978;
232 10.1021/es3025319.
- 233 3. Heald, C.L.; Collett, J.L., Jr.; Lee, T.; Benedict, K.B.; Schwandner, F.M.; Li, Y.; Clarisse, L.;
234 Hurtmans, D.R.; Van Damme, M.; Clerbaux, C.; Coheur, P.-.; Philip, S.; Martin, R.V.; Pye,
235 H.O.T. Atmospheric ammonia and particulate inorganic nitrogen over the United States.
236 *Atmospheric Chemistry and Physics* **2012**, 12 (21), 10295-10312; 10.5194/acp-12-10295-2012.
- 237 4. Walker, J.M.; Philip, S.; Martin, R.V.; Seinfeld, J.H. Simulation of nitrate, sulfate, and
238 ammonium aerosols over the United States. *Atmospheric Chemistry and Physics* **2012**, 12 (22),
239 11213-11227; 10.5194/acp-12-11213-2012.
- 240 5. Bey, I.; Jacob, D.J.; Yantosca, R.M.; Logan, J.A.; Field, B.D.; Fiore, A.M.; Li, Q.B.; Liu,
241 H.G.Y.; Mickley, L.J.; Schultz, M.G. Global modeling of tropospheric chemistry with
242 assimilated meteorology: Model description and evaluation. *Journal of Geophysical Research-
243 Atmospheres* **2001**, 106 (D19); 10.1029/2001JD000807.
- 244 6. Park, R.J.; Jacob, D.J.; Field, B.D.; Yantosca, R.M.; Chin, M. Natural and transboundary
245 pollution influences on sulfate-nitrate-ammonium aerosols in the United States: Implications for
246 policy. *Journal of Geophysical Research-Atmospheres* **2004**, 109 (D15), D15204;
247 10.1029/2003JD004473.
- 248 7. Martin, R. V.; Jacob, D.J.; Yantosca, R.M.; Chin, M.; Ginoux, P. Global and regional
249 decreases in tropospheric oxidants from photochemical effects of aerosols. *Journal of
250 Geophysical Research-Atmospheres* **2003**, 108 (D3), 4097; 10.1029/2002JD002622.
- 251 8. Jacob, D.J. Heterogeneous chemistry and tropospheric ozone. *Atmos. Environ.* **2000**, 34 (12-
252 14), 2131-2159; 10.1016/S1352-2310(99)00462-8.
- 253 9. Evans, M.J. and Jacob, D.J. Impact of new laboratory studies of N₂O₅ hydrolysis on global
254 model budgets of tropospheric nitrogen oxides, ozone, and OH. *Geophys. Res. Lett.* **2005**, 32 (9),
255 L09813; 10.1029/2005GL022469.

- 256 10. Thornton, J.A.; Jaegle, L.; McNeill, V.F. Assessing known pathways for HO₂ loss in
257 aqueous atmospheric aerosols: Regional and global impacts on tropospheric oxidants. *Journal of*
258 *Geophysical Research-Atmospheres* **2008**, 113 (D5), D05303; 10.1029/2007JD009236.
- 259 11. Fountoukis, C. and Nenes, A. ISORROPIA II: a computationally efficient thermodynamic
260 equilibrium model for K⁺-Ca²⁺-Mg²⁺-NH₄(+)-Na⁺-SO₄²⁻-NO₃⁻-Cl⁻-H₂O aerosols.
261 *Atmospheric Chemistry and Physics* **2007**, 7 (17).
- 262 12. Pye, H.O.T.; Liao, H.; Wu, S.; Mickley, L.J.; Jacob, D.J.; Henze, D.K.; Seinfeld, J.H. Effect
263 of changes in climate and emissions on future sulfate-nitrate-ammonium aerosol levels in the
264 United States. *Journal of Geophysical Research-Atmospheres* **2009**, 114, D01205;
265 10.1029/2008JD010701.
- 266 13. Fisher, J.A.; Jacob, D.J.; Wang, Q.; Bahreini, R.; Carouge, C.C.; Cubison, M.J.; Dibb, J.E.;
267 Diehl, T.; Jimenez, J.L.; Leibensperger, E.M.; Lu, Z.; Meinders, M.B.J.; Pye, H.O.T.; Quinn,
268 P.K.; Sharma, S.; Streets, D.G.; van Donkelaar, A.; Yantosca, R.M. Sources, distribution, and
269 acidity of sulfate-ammonium aerosol in the Arctic in winter-spring. *Atmos. Environ.* **2011**, 45
270 (39), 7301-7318; 10.1016/j.atmosenv.2011.08.030.
- 271 14. Ridley, D.A.; Heald, C.L.; Ford, B. North African dust export and deposition: A satellite and
272 model perspective. *Journal of Geophysical Research-Atmospheres* **2012**, 117, D02202;
273 10.1029/2011JD016794.
- 274 15. Kuhns, H.; Knipping, E.M.; Vukovich, J.M. Development of a United States-Mexico
275 emissions inventory for the Big Bend Regional Aerosol and Visibility Observational (BRAVO)
276 Study. *J. Air Waste Manage. Assoc.* **2005**, 55 (5), 677-692.
- 277 16. Zhang, Q.; Streets, D.G.; Carmichael, G.R.; He, K.B.; Huo, H.; Kannari, A.; Klimont, Z.;
278 Park, I.S.; Reddy, S.; Fu, J.S.; Chen, D.; Duan, L.; Lei, Y.; Wang, L.T.; Yao, Z.L. Asian
279 emissions in 2006 for the NASA INTEX-B mission. *Atmospheric Chemistry and Physics* **2009**,
280 9 (14), 5131-5153.
- 281 17. Lu, Z.; Zhang, Q.; Streets, D.G. Sulfur dioxide and primary carbonaceous aerosol emissions
282 in China and India, 1996-2010. *Atmospheric Chemistry and Physics* **2011**, 11 (18), 9839-9864;
283 10.5194/acp-11-9839-2011.
- 284 18. Olivier JGJ, e.a. Recent trends in global greenhouse gas emissions: regional trends 1970-
285 2000 and spatial distribution of key sources in 2000. *Env. Sc.* **2005**, 2 (2-3), 81-99;
286 10.1080/15693430500400345.
- 287 19. van Donkelaar, A.; Martin, R.V.; Leaitch, W.R.; Macdonald, A.M.; Walker, T.W.; Streets,
288 D.G.; Zhang, Q.; Dunlea, E.J.; Jimenez, J.L.; Dibb, J.E.; Huey, L.G.; Weber, R.; Andreae, M.O.
289 Analysis of aircraft and satellite measurements from the Intercontinental Chemical Transport
290 Experiment (INTEX-B) to quantify long-range transport of East Asian sulfur to Canada.
291 *Atmospheric Chemistry and Physics* **2008**, 8 (11).

- 292 20. Lamsal, L.N.; Martin, R.V.; Padmanabhan, A.; van Donkelaar, A.; Zhang, Q.; Sioris, C.E.;
293 Chance, K.; Kurosu, T.P.; Newchurch, M.J. Application of satellite observations for timely
294 updates to global anthropogenic NO_x emission inventories. *Geophys. Res. Lett.* **2011**, *38*,
295 L05810; 10.1029/2010GL046476.
- 296 21. Yienger, J.J. and Levy, H. Empirical-Model of Global Soil-Biogenic NO_x Emissions. *Journal*
297 *of Geophysical Research-Atmospheres* **1995**, *100* (D6), 11447-11464; 10.1029/95JD00370.
- 298 22. Wang, Y.H.; Jacob, D.J.; Logan, J.A. Global simulation of tropospheric O₃-NO_x-
299 hydrocarbon chemistry 1. Model formulation. *Journal of Geophysical Research-Atmospheres*
300 **1998**, *103* (D9), 10713-10725; 10.1029/98JD00158.
- 301 23. Price, C. and Rind, D. A Simple Lightning Parameterization for Calculating Global
302 Lightning Distributions. *Journal of Geophysical Research-Atmospheres* **1992**, *97* (D9), 9919-
303 9933.
- 304 24. Sauvage, B.; Martin, R.V.; van Donkelaar, A.; Ziemke, J.R. Quantification of the factors
305 controlling tropical tropospheric ozone and the South Atlantic maximum. *Journal of Geophysical*
306 *Research-Atmospheres* **2007**, *112* (D11), D11309; 10.1029/2006JD008008.
- 307 25. Martin, R.V.; Sauvage, B.; Folkins, I.; Sioris, C.E.; Boone, C.; Bernath, P.; Ziemke, J. Space-
308 based constraints on the production of nitric oxide by lightning. *Journal of Geophysical*
309 *Research-Atmospheres* **2007**, *112* (D9), D09309; 10.1029/2006JD007831.
- 310 26. Hudman, R.C.; Jacob, D.J.; Turquety, S.; Leibensperger, E.M.; Murray, L.T.; Wu, S.;
311 Gilliland, A.B.; Avery, M.; Bertram, T.H.; Brune, W.; Cohen, R.C.; Dibb, J.E.; Flocke, F.M.;
312 Fried, A.; Holloway, J.; Neuman, J.A.; Orville, R.; Perring, A.; Ren, X.; Sachse, G.W.; Singh,
313 H.B.; Swanson, A.; Wooldridge, P.J. Surface and lightning sources of nitrogen oxides over the
314 United States: Magnitudes, chemical evolution, and outflow. *Journal of Geophysical Research-
315 Atmospheres* **2007**, *112* (D12), D12S05; 10.1029/2006JD007912.
- 316 27. Murray, L.T.; Jacob, D.J.; Logan, J.A.; Hudman, R.C.; Koshak, W.J. Optimized regional and
317 interannual variability of lightning in a global chemical transport model constrained by LIS/OTD
318 satellite data. *Journal of Geophysical Research-Atmospheres* **2012**, *117*, D20307;
319 10.1029/2012JD017934.
- 320 28. Lee, C.; Martin, R.V.; van Donkelaar, A.; Lee, H.; Dickerson, R.R.; Hains, J.C.; Krotkov, N.;
321 Richter, A.; Vinnikov, K.; Schwab, J.J. SO₂ emissions and lifetimes: Estimates from inverse
322 modeling using in situ and global, space-based (SCIAMACHY and OMI) observations. *Journal*
323 *of Geophysical Research-Atmospheres* **2011**, *116*, D06304; 10.1029/2010JD014758.
- 324 29. Vinken, G.C.M.; Boersma, K.F.; Jacob, D.J.; Meijer, E.W. Accounting for non-linear
325 chemistry of ship plumes in the GEOS-Chem global chemistry transport model. *Atmospheric*
326 *Chemistry and Physics* **2011**, *11* (22), 11707-11722; 10.5194/acp-11-11707-2011.

- 327 30. Bouwman, A.F.; Lee, D.S.; Asman, W.A.H.; Dentener, F.J.; VanderHoek, K.W.; Olivier,
328 J.G.J. A global high-resolution emission inventory for ammonia. Global Biogeochem. Cycles
329 **1997**, 11 (4), 561-587; 10.1029/97GB02266.
- 330 31. Sheppard, S.C.; Bittman, S.; Swift, M.L.; Tait, J. Modelling monthly NH₃ emissions from
331 dairy in 12 Ecoregions of Canada. Canadian Journal of Animal Science **2011**, 91 (4), 649-661;
332 10.4141/CJAS2010-005.
- 333 32. Streets, D.G.; Bond, T.C.; Carmichael, G.R.; Fernandes, S.D.; Fu, Q.; He, D.; Klimont, Z.;
334 Nelson, S.M.; Tsai, N.Y.; Wang, M.Q.; Woo, J.H.; Yarber, K.F. An inventory of gaseous and
335 primary aerosol emissions in Asia in the year 2000. Journal of Geophysical Research-
336 Atmospheres **2003**, 108 (D21), 8809; 10.1029/2002JD003093.
- 337 33. Kharol, S.K.; Martin, R.V.; Philip, S.; Vogel, S.; Henze, D.K.; Chen, D.; Wang, Y.; Zhang,
338 Q.; Heald, C.L. Persistent sensitivity of Asian aerosol to emissions of nitrogen oxides. Geophys.
339 Res. Lett. **2013**, 40 (5), 1021-1026; 10.1002/grl.50234.
- 340 34. Huang, K.; Zhuang, G.; Lin, Y.; Fu, J.S.; Wang, Q.; Liu, T.; Zhang, R.; Jiang, Y.; Deng, C.;
341 Fu, Q.; Hsu, N.C.; Cao, B. Typical types and formation mechanisms of haze in an Eastern Asia
342 megacity, Shanghai. Atmospheric Chemistry and Physics **2012**, 12 (1), 105-124; 10.5194/acp-
343 12-105-2012.
- 344 35. Huang, X.; Song, Y.; Li, M.; Li, J.; Huo, Q.; Cai, X.; Zhu, T.; Hu, M.; Zhang, H. A high-
345 resolution ammonia emission inventory in China. Global Biogeochem. Cycles **2012**, 26,
346 GB1030; 10.1029/2011GB004161.
- 347 36. Park, R.J.; Jacob, D.J.; Chin, M.; Martin, R.V. Sources of carbonaceous aerosols over the
348 United States and implications for natural visibility. Journal of Geophysical Research-
349 Atmospheres **2003**, 108 (D12), 4355; 10.1029/2002JD003190.
- 350 37. Wang, Q.; Jacob, D.J.; Fisher, J.A.; Mao, J.; Leibensperger, E.M.; Carouge, C.C.; Le Sager,
351 P.; Kondo, Y.; Jimenez, J.L.; Cubison, M.J.; Doherty, S.J. Sources of carbonaceous aerosols and
352 deposited black carbon in the Arctic in winter-spring: implications for radiative forcing.
353 Atmospheric Chemistry and Physics **2011**, 11 (23), 12453-12473; 10.5194/acp-11-12453-2011.
- 354 38. Bond, T.C.; Bhardwaj, E.; Dong, R.; Jogani, R.; Jung, S.; Roden, C.; Streets, D.G.;
355 Trautmann, N.M. Historical emissions of black and organic carbon aerosol from energy-related
356 combustion, 1850-2000. Global Biogeochem. Cycles **2007**, 21 (2), GB2018;
357 10.1029/2006GB002840.
- 358 39. Cooke, W.F.; Liousse, C.; Cachier, H.; Feichter, J. Construction of a 1 degrees x 1 degrees
359 fossil fuel emission data set for carbonaceous aerosol and implementation and radiative impact in
360 the ECHAM4 model. Journal of Geophysical Research-Atmospheres **1999**, 104 (D18);
361 10.1029/1999JD900187.

- 362 40. Leibensperger, E.M.; Mickley, L.J.; Jacob, D.J.; Chen, W.-.; Seinfeld, J.H.; Nenes, A.;
363 Adams, P.J.; Streets, D.G.; Kumar, N.; Rind, D. Climatic effects of 1950-2050 changes in US
364 anthropogenic aerosols - Part 1: Aerosol trends and radiative forcing. *Atmospheric Chemistry*
365 and Physics
- 366 41. Fu, T.-.; Cao, J.J.; Zhang, X.Y.; Lee, S.C.; Zhang, Q.; Han, Y.M.; Qu, W.J.; Han, Z.; Zhang,
367 R.; Wang, Y.X.; Chen, D.; Henze, D.K. Carbonaceous aerosols in China: top-down constraints
368 on primary sources and estimation of secondary contribution. *Atmospheric Chemistry and*
369 *Physics* **2012**, 12 (7); 10.5194/acp-12-3333-2012.
- 370 42. Wang, X.; Wang, Y.; Hao, J.; Kondo, Y.; Irwin, M.; Munger, J.W.; Zhao, Y. Top-down
371 estimate of China's black carbon emissions using surface observations: Sensitivity to observation
372 representativeness and transport model error. *Journal of Geophysical Research: Atmospheres*
373 **2013**, 118 (11), 5781-5795; 10.1002/jgrd.50397.
- 374 43. Henze, D.K. and Seinfeld, J.H. Global secondary organic aerosol from isoprene oxidation.
375 *Geophys. Res. Lett.* **2006**, 33 (9), L09812; 10.1029/2006GL025976.
- 376 44. Henze, D.K.; Seinfeld, J.H.; Ng, N.L.; Kroll, J.H.; Fu, T.-.; Jacob, D.J.; Heald, C.L. Global
377 modeling of secondary organic aerosol formation from aromatic hydrocarbons: high- vs. low-
378 yield pathways. *Atmospheric Chemistry and Physics* **2008**, 8 (9).
- 379 45. Liao, H.; Henze, D.K.; Seinfeld, J.H.; Wu, S.; Mickley, L.J. Biogenic secondary organic
380 aerosol over the United States: Comparison of climatological simulations with observations.
381 *Journal of Geophysical Research-Atmospheres* **2007**, 112 (D6), D06201;
382 10.1029/2006JD007813.
- 383 46. Fu, T.; Jacob, D.J.; Wittrock, F.; Burrows, J.P.; Vrekoussis, M.; Henze, D.K. Global budgets
384 of atmospheric glyoxal and methylglyoxal, and implications for formation of secondary organic
385 aerosols. *Journal of Geophysical Research-Atmospheres* **2008**, 113 (D15), D15303;
386 10.1029/2007JD009505.
- 387 47. van der Werf, G.R.; Randerson, J.T.; Giglio, L.; Collatz, G.J.; Mu, M.; Kasibhatla, P.S.;
388 Morton, D.C.; DeFries, R.S.; Jin, Y.; van Leeuwen, T.T. Global fire emissions and the
389 contribution of deforestation, savanna, forest, agricultural, and peat fires (1997-2009).
390 *Atmospheric Chemistry and Physics* **2010**, 10 (23), 11707-11735; 10.5194/acp-10-11707-2010.
- 391 48. Mu, M.; Randerson, J.T.; van der Werf, G.R.; Giglio, L.; Kasibhatla, P.; Morton, D.; Collatz,
392 G.J.; DeFries, R.S.; Hyer, E.J.; Prins, E.M.; Griffith, D.W.T.; Wunch, D.; Toon, G.C.; Sherlock,
393 V.; Wennberg, P.O. Daily and 3-hourly variability in global fire emissions and consequences for
394 atmospheric model predictions of carbon monoxide. *Journal of Geophysical Research-
395 Atmospheres* **2011**, 116, D24303; 10.1029/2011JD016245.
- 396 49. Yevich, R. and Logan, J.A. An assessment of biofuel use and burning of agricultural waste in
397 the developing world. *Global Biogeochem. Cycles* **2003**, 17 (4), 1095; 10.1029/2002GB001952.

- 398 50. Philip, S.; Martin, R.V.; Pierce, J.R.; Jimenez, J.L.; Zhang, Q.; Canagaratna, M.R.;
399 Spracklen, D.V.; Nowlan, C.R.; Lamsal, L.N.; Cooper, M.J.; Krotkov, N.A. Spatially and
400 seasonally resolved estimate of the ratio of organic mass to organic carbon. *Atmos. Environ.*
401 **2014**, 87 (0), 34-40; <http://dx.doi.org/10.1016/j.atmosenv.2013.11.065>.
- 402 51. Fairlie, T.D.; Jacob, D.J.; Park, R.J. The impact of transpacific transport of mineral dust in
403 the United States. *Atmos. Environ.* **2007**, 41 (6); 10.1016/j.atmosenv.2006.09.048.
- 404 52. Alexander, B.; Park, R.J.; Jacob, D.J.; Li, Q.B.; Yantosca, R.M.; Savarino, J.; Lee, C.C.W.;
405 Thiemens, M.H. Sulfate formation in sea-salt aerosols: Constraints from oxygen isotopes.
406 *Journal of Geophysical Research-Atmospheres* **2005**, 110 (D10), D10307;
407 10.1029/2004JD005659.
- 408 53. Jaegle, L.; Quinn, P.K.; Bates, T.S.; Alexander, B.; Lin, J.-. Global distribution of sea salt
409 aerosols: new constraints from in situ and remote sensing observations. *Atmospheric Chemistry*
410 and Physics **2011**, 11 (7), 3137-3157; 10.5194/acp-11-3137-2011.
- 411 54. Liu, H.Y.; Jacob, D.J.; Bey, I.; Yantosca, R.M. Constraints from Pb-210 and Be-7 on wet
412 deposition and transport in a global three-dimensional chemical tracer model driven by
413 assimilated meteorological fields. *Journal of Geophysical Research-Atmospheres* **2001**, 106
414 (D11), 12109-12128; 10.1029/2000JD900839.
- 415 55. Amos, H.M.; Jacob, D.J.; Holmes, C.D.; Fisher, J.A.; Wang, Q.; Yantosca, R.M.; Corbitt,
416 E.S.; Galarneau, E.; Rutter, A.P.; Gustin, M.S.; Steffen, A.; Schauer, J.J.; Graydon, J.A.; St
417 Louis, V.L.; Talbot, R.W.; Edgerton, E.S.; Zhang, Y.; Sunderland, E.M. Gas-particle partitioning
418 of atmospheric Hg(II) and its effect on global mercury deposition. *Atmospheric Chemistry and*
419 *Physics* **2012**, 12 (1), 591-603; 10.5194/acp-12-591-2012.
- 420 56. Park, R.J.; Jacob, D.J.; Kumar, N.; Yantosca, R.M. Regional visibility statistics in the United
421 States: Natural and transboundary pollution influences, and implications for the Regional Haze
422 Rule. *Atmos. Environ.* **2006**, 40 (28); 10.1016/j.atmosenv.2006.04.059.
- 423 57. Zhang, L.; Jacob, D.J.; Knipping, E.M.; Kumar, N.; Munger, J.W.; Carouge, C.C.; van
424 Donkelaar, A.; Wang, Y.X.; Chen, D. Nitrogen deposition to the United States: distribution,
425 sources, and processes. *Atmospheric Chemistry and Physics* **2012**, 12 (10); 10.5194/acp-12-
426 4539-2012.
- 427 58. Drury, E.; Jacob, D.J.; Spurr, R.J.D.; Wang, J.; Shinozuka, Y.; Anderson, B.E.; Clarke, A.D.;
428 Dibb, J.; McNaughton, C.; Weber, R. Synthesis of satellite (MODIS), aircraft (ICARTT), and
429 surface (IMPROVE, EPA-AQS, AERONET) aerosol observations over eastern North America
430 to improve MODIS aerosol retrievals and constrain surface aerosol concentrations and sources.
431 *Journal of Geophysical Research-Atmospheres* **2010**, 115, D14204; 10.1029/2009JD012629.
- 432 59. Heald, C.L.; Coe, H.; Jimenez, J.L.; Weber, R.J.; Bahreini, R.; Middlebrook, A.M.; Russell,
433 L.M.; Jolley, M.; Fu, T.-.; Allan, J.D.; Bower, K.N.; Capes, G.; Crosier, J.; Morgan, W.T.;

- 434 Robinson, N.H.; Williams, P.I.; Cubison, M.J.; DeCarlo, P.F.; Dunlea, E.J. Exploring the vertical
435 profile of atmospheric organic aerosol: comparing 17 aircraft field campaigns with a global
436 model. *Atmospheric Chemistry and Physics* **2011**, 11 (24), 12673-12696; 10.5194/acp-11-
437 12673-2011.
- 438 60. van Donkelaar, A.; Martin, R.V.; Brauer, M.; Kahn, R.; Levy, R.; Verduzco, C.; Villeneuve,
439 P.J. Global Estimates of Ambient Fine Particulate Matter Concentrations from Satellite-Based
440 Aerosol Optical Depth: Development and Application. *Environ. Health Perspect.* **2010**, 118 (6);
441 10.1289/ehp.0901623.
- 442 61. van Donkelaar, A.; Martin, R.V.; Spurr, R.J.D.; Drury, E.; Remer, L.A.; Levy, R.C.; Wang,
443 J. Optimal estimation for global ground-level fine particulate matter concentrations. *Journal of*
444 *Geophysical Research: Atmospheres* **2013**, 118 (11), 5621-5636; 10.1002/jgrd.50479.
- 445 62. Ford, B. and Heald, C.L. An A-train and model perspective on the vertical distribution of
446 aerosols and CO in the Northern Hemisphere. *Journal of Geophysical Research-Atmospheres*
447 **2012**, 117, D06211; 10.1029/2011JD016977.
- 448 63. Dabek-Zlotorzynska, E.; Dann, T.F.; Martinelango, P.K.; Celo, V.; Brook, J.R.; Mathieu, D.;
449 Ding, L.; Austin, C.C. Canadian National Air Pollution Surveillance (NAPS) PM2.5 speciation
450 program: Methodology and PM2.5 chemical composition for the years 2003-2008. *Atmos.*
451 *Environ.* **2011**, 45 (3); 10.1016/j.atmosenv.2010.10.024.
- 452 64. Zhang, L.; Vet, R.; Wiebe, A.; Mihele, C.; Sukloff, B.; Chan, E.; Moran, M.D.; Iqbal, S.
453 Characterization of the size-segregated water-soluble inorganic ions at eight Canadian rural sites.
454 *Atmospheric Chemistry and Physics* **2008**, 8 (23).
- 455 65. Hand JL, e.a. IMPROVE (Interagency Monitoring of Protected Visual Environments):
456 Spatial and seasonal patterns and temporal variability of haze and its constituents in the United
457 States. **2011**, Rep. V, Coop. Inst. For Res. In the Atmos., Fort Collins, Colo., .
- 458 66. Rattigan, O.V.; Felton, H.D.; Bae, M.; Schwab, J.J.; Demerjian, K.L. Comparison of long-
459 term PM2.5 carbon measurements at an urban and rural location in New York. *Atmos. Environ.*
460 **2011**, 45 (19); 10.1016/j.atmosenv.2011.03.048.
- 461 67. Turpin, B.J. and Lim, H.J. Species contributions to PM2.5 mass concentrations: Revisiting
462 common assumptions for estimating organic mass. *Aerosol Science and Technology* **2001**, 35
463 (1); 10.1080/02786820152051454.
- 464 68. Simon, H.; Bhawe, P.V.; Swall, J.L.; Frank, N.H.; Malm, W.C. Determining the spatial and
465 seasonal variability in OM/OC ratios across the US using multiple regression. *Atmospheric*
466 *Chemistry and Physics* **2011**, 11 (6); 10.5194/acp-11-2933-2011.

- 467 69. Malm, W.C.; Sisler, J.F.; Huffman, D.; Eldred, R.A.; Cahill, T.A. Spatial and Seasonal
468 Trends in Particle Concentration and Optical Extinction in the United-States. *Journal of*
469 *Geophysical Research-Atmospheres* **1994**, 99 (D1), 1347-1370; 10.1029/93JD02916.
- 470 70. Malm, W.C. and Hand, J.L. An examination of the physical and optical properties of aerosols
471 collected in the IMPROVE program. *Atmos. Environ.* **2007**, 41 (16);
472 10.1016/j.atmosenv.2006.12.012.
- 473 71. White, W.H. Chemical markers for sea salt in IMPROVE aerosol data. *Atmos. Environ.*
474 **2008**, 42 (2); 10.1016/j.atmosenv.2007.09.040.
- 475 72. Hand, J.L.; Schichtel, B.A.; Pitchford, M.; Malm, W.C.; Frank, N.H. Seasonal composition
476 of remote and urban fine particulate matter in the United States. *Journal of Geophysical*
477 *Research-Atmospheres* **2012**, 117, D05209; 10.1029/2011JD017122.
- 478 73. Zhang, X.Y.; Wang, Y.Q.; Zhang, X.C.; Guo, W.; Gong, S.L. Carbonaceous aerosol
479 composition over various regions of China during 2006. *Journal of Geophysical Research-*
480 *Atmospheres* **2008**, 113 (D14), D14111; 10.1029/2007JD009525.
- 481 74. Cao, J.J.; Lee, S.C.; Chow, J.C.; Watson, J.G.; Ho, K.F.; Zhang, R.J.; Jin, Z.D.; Shen, Z.X.;
482 Chen, G.C.; Kang, Y.M.; Zou, S.C.; Zhang, L.Z.; Qi, S.H.; Dai, M.H.; Cheng, Y.; Hu, K. Spatial
483 and seasonal distributions of carbonaceous aerosols over China. *Journal of Geophysical*
484 *Research-Atmospheres* **2007**, 112 (D22), D22S11; 10.1029/2006JD008205.
- 485 75. Yang, F.; Tan, J.; Zhao, Q.; Du, Z.; He, K.; Ma, Y.; Duan, F.; Chen, G.; Zhao, Q.
486 Characteristics of PM2.5 speciation in representative megacities and across China. *Atmospheric*
487 *Chemistry and Physics* **2011**, 11 (11); 10.5194/acp-11-5207-2011.
- 488 76. So, K.L.; Guo, H.; Li, Y.S. Long-term variation of PM2.5 levels and composition at rural,
489 urban, and roadside sites in Hong Kong: Increasing impact of regional air pollution. *Atmos.*
490 *Environ.* **2007**, 41 (40); 10.1016/j.atmosenv.2007.08.053.
- 491 77. Chowdhury M. Characterization of fine particle air pollution in the Indian subcontinent. PhD
492 Thesis, Georgia Institute of Technology, USA. **2004**.
- 493 78. Stone, E.; Schauer, J.; Quraishi, T.A.; Mahmood, A. Chemical characterization and source
494 apportionment of fine and coarse particulate matter in Lahore, Pakistan. *Atmos. Environ.* **2010**,
495 44 (8); 10.1016/j.atmosenv.2009.12.015.
- 496 79. Soluri, D.S.; Godoy, M.L.D.P.; Godoy, J.M.; Roldao, L.A. Multi-site PM2.5 and PM2.5-10
497 aerosol source apportionment in Rio de Janeiro, Brazil. *Journal of the Brazilian Chemical*
498 *Society* **2007**, 18 (4).
- 499 80. Sarnat, J.A.; Moise, T.; Shpund, J.; Liu, Y.; Pachon, J.E.; Qasrawi, R.; Abdeen, Z.; Brenner,
500 S.; Nassar, K.; Saleh, R.; Schauer, J.J. Assessing the spatial and temporal variability of fine

- 501 particulate matter components in Israeli, Jordanian, and Palestinian cities. *Atmos. Environ.* **2010**,
502 44 (20); 10.1016/j.atmosenv.2010.04.007.
- 503 81. Pey, J.; Querol, X.; Alastuey, A. Variations of levels and composition of PM10 and PM2.5 at
504 an insular site in the Western Mediterranean. *Atmos. Res.* **2009**, 94 (2);
505 10.1016/j.atmosres.2009.06.006.
- 506 82. Brown, K.W.; Bouhamra, W.; Lamoureux, D.P.; Evans, J.S.; Koutrakis, P. Characterization
507 of particulate matter for three sites in Kuwait. *J. Air Waste Manage. Assoc.* **2008**, 58 (8);
508 10.3155/1047-3289.58.8.994.
- 509 83. Zhang, X.Y.; Wang, Y.Q.; Niu, T.; Zhang, X.C.; Gong, S.L.; Zhang, Y.M.; Sun, J.Y.
510 Atmospheric aerosol compositions in China: spatial/temporal variability, chemical signature,
511 regional haze distribution and comparisons with global aerosols. *Atmospheric Chemistry and*
512 *Physics* **2012**, 12 (2); 10.5194/acp-12-779-2012.
- 513 84. Qu, W.J.; Zhang, X.Y.; Arimoto, R.; Wang, D.; Wang, Y.Q.; Yan, L.W.; Li, Y. Chemical
514 composition of the background aerosol at two sites in southwestern and northwestern China:
515 potential influences of regional transport. *Tellus Series B-Chemical and Physical Meteorology*
516 **2008**, 60 (4), 657-673; 10.1111/j.1600-0889.2008.00342-x.
- 517 85. Qu, W.; Zhang, X.; Arimoto, R.; Wang, Y.; Wang, D.; Sheng, L.; Fu, G. Aerosol background
518 at two remote CAWNET sites in western China. *Sci. Total Environ.* **2009**, 407 (11);
519 10.1016/j.scitotenv.2009.02.012.